Volume 30
Number 7
April 3, 1991

Inorganic Chemistry

Communications

Thermodynamics of Multielectron Transfer: Variable-Temperature UV-Vis and IR Spectroelectrochemical Studies of the Disproportionation of d^7–d^8 Binuclear Rhodium Complexes

Transition-metal complexes capable of multiple-electron-transfer reactions have received considerable attention in recent years.[1-7] The ultimate goal of this research is to design multielectron-transfer reagents for the production of useful molecules such as H_2 and $C_2O_4^{2-}$ by avoiding high-energy intermediates formed in sequential one-electron processes.[8,9]

Our work in this area has focused on bridged, binuclear complexes of rhodium(I) and iridium(I) (see Chart I), in which the two metal centers are held together by diisocyanide ligands. Like other d^8–d^8 chromophores,[4,5] these complexes undergo facile redox reactions, which implicate them as potential electron-transfer catalysts.[10] For example, numerous electrochemical experiments[7,11] have shown that a variety of binuclear d^8–d^8 precursors give rise to net two-electron oxidation products at moderate potentials, via chemically reversible processes.

Chart I. Diagrams for Binuclear Rh(I) Complexes

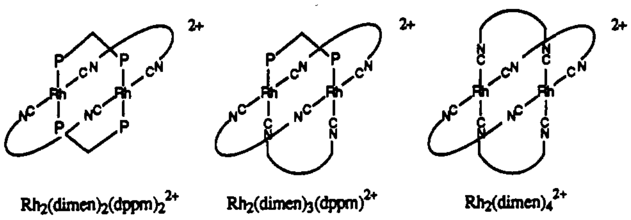

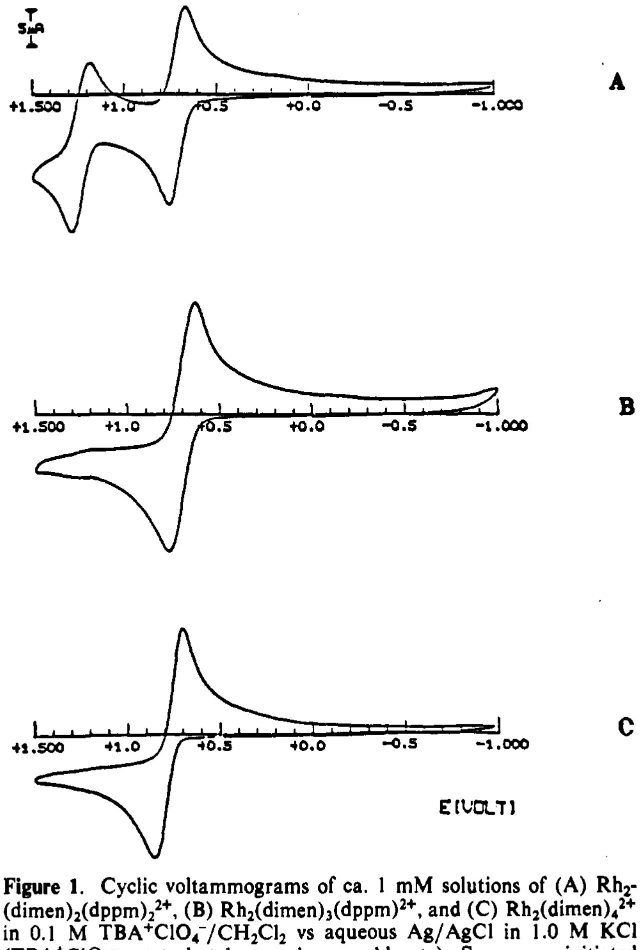

Figure 1. Cyclic voltammograms of ca. 1 mM solutions of (A) $Rh_2(dimen)_2(dppm)_2^{2+}$, (B) $Rh_2(dimen)_3(dppm)^{2+}$, and (C) $Rh_2(dimen)_4^{2+}$ in 0.1 M $TBA^+ClO_4^-/CH_2Cl_2$ vs aqueous Ag/AgCl in 1.0 M KCl ($TBA^+ClO_4^-$ = tetrabutylammonium perchlorate). Scans were initiated in the positive direction, at a rate of 100 mV/s. In each case, $i_{p,c}/i_{p,a}$ = 1 ± 0.05.

Whether the d^7–d^7 oxidation product is formed by two sequential $1e^-$ steps or by a single net $2e^-$ process is a matter of considerable practical importance. It depends intimately both on the relative thermodynamic stabilities of the d^8–d^8, d^7–d^8, and d^7–d^7 oxidation states and on the barriers to their interconversion. The relative thermodynamic stabilities, in turn, are sensitive to structural changes and medium effects;[12] however, the lack of thermodynamic data, particularly for d^7–d^8 transient intermediates, has left the precise nature of these effects largely unexplored.

As a first step toward unraveling these phenomena, we have applied variable-temperature spectroelectrochemical techniques

---

(1) Kalyanasundaram, K.; Gratzel, M.; Pelizzetti, E. *Coord. Chem. Rev.* **1986**, *69*, 67.

(2) (a) Chang, I. J.; Nocera, D. G. *J. Am. Chem. Soc.* **1987**, *109*, 4901. (b) Chang, I. J.; Nocera, D. G. *Inorg. Chem.* **1989**, *28*, 4309.

(3) Partigianoni, C. M.; Nocera, D. G. *Inorg. Chem.* **1990**, *29*, 2033.

(4) Roundhill, D. M.; Gray, H. B.; Che, C. M. *Acc. Chem. Res.* **1989**, *22*, 55.

(5) Marshall, J. L.; Steigman, A. E.; Gray, H. B. In *Excited States and Reactive Intermediates*; Lever, A. P. B., Ed.; ACS Symposium Series 307; American Chemical Society: Washington, DC, 1986; p 166.

(6) Mann, K. R.; Lewis, N. S.; Miskowski, V. M.; Erwin, D. K.; Hammond, G. S.; Gray, H. B. *J. Am. Chem. Soc.* **1977**, *99*, 5525.

(7) Rhodes, M. R.; Mann, K. R. *Inorg. Chem.* **1984**, *23*, 2053.

(8) (a) Sutin, N.; Creutz, C. *Pure Appl. Chem.* **1980**, *52*, 2717. (b) Graetzel, M., Ed. *Energy Resources through Photochemistry and Catalysis*, Academic Press: New York, 1983; and references therein.

(9) (a) Eisenberg, R.; Hendrickson, D. E. *Adv. Catal.* **1979**, *28*, 79. (b) O'Toole, T. R.; Margerum, L. D.; Westmoreland, T. D.; Vining, W. J.; Murray, R. W.; Meyer, T. J. *J. Chem. Soc., Chem. Commun.* **1985**, 1416. (c) Hawecker, J.; Lehn, J.-M.; Ziessel, R. *Helv. Chim. Acta* **1986**, *69*, 1990.

(10) Gray, H. B.; Miskowski, V. M.; Milder, S. J.; Smith, T. P.; Maverick, A. W.; Buhr, J. D.; Gladfelter, W. L.; Segal, I. S.; Mann, K. R. *Fundam. Res. Homogeneous Catal.* **1979**, *3*, 819.

(11) (a) Boyd, D. C.; Matsch, P. A.; Mixa, M. M.; Mann, K. R. *Inorg. Chem.* **1986**, *25*, 3331. (b) Womack, D. R.; Enlow, P. D.; Woods, C. *Inorg. Chem.* **1983**, *22*, 2653. (c) Tortorelli, L. J.; Woods, C.; McPhail, A. T. *Inorg. Chem.* **1990**, *29*, 2726.

(12) Boyd, D. C.; Rodman, G. S.; Mann, K. R. *J. Am. Chem. Soc.* **1986**, *108*, 1779.

0020-1669/91/1330-1429$02.50/0 © 1991 American Chemical Society

to obtain thermodynamic parameters for the d^8–d^8, d^7–d^8, and d^7–d^7 electronic states of a series of binuclear rhodium complexes: $[Rh_2(dimen)_2(dppm)_2][PF_6]_2$,[11a] $[Rh_2(dimen)_3(dppm)][PF_6]_2$,[13] and $[Rh_2(dimen)_4][PF_6]_2$[7] (where dimen = 1,8-diisocyanomenthane and dppm = bis(diphenylphosphino)methane). These structurally similar complexes display a remarkable variation for undergoing 1e⁻ vs 2e⁻ oxidations and provide an ideal opportunity to discern the subtle electronic and structural features that control single vs multielectron transfers.

Cyclic voltammograms for the three complexes are shown in Figure 1. As previously reported,[11a] $Rh_2(dimen)_2(dppm)_2^{2+}$ shows two successive quasi-reversible 1e⁻ oxidations at +0.700 and +1.226 V. In contrast, $Rh_2(dimen)_3(dppm)^{2+}$ and $Rh_2(dimen)_4^{2+}$ each display single, quasi-reversible 2e⁻ oxidations, centered at +0.710 and +0.780 V, respectively.[7,16]

As noted above, the thermodynamic driving force for a 2e⁻ transfer is related to the relative stabilities of the d^8–d^8, d^7–d^8, and d^7–d^7 electronic configurations. Electrochemically, these stabilities are expressed in the formal single-electron redox couples, $E^{\circ\prime}_{3+/2+}$ and $E^{\circ\prime}_{4+/3+}$.[17] While cyclic voltammetry provides these potentials directly for $Rh_2(dimen)_2(dppm)_2^{2+}$, it yields only the potentials of the apparent two-electron couple, $E^{\circ\prime}_{4+/2+}$, for $Rh_2(dimen)_3(dppm)^{2+}$ and $Rh_2(dimen)_4^{2+}$. We can, however, calculate the necessary one-electron potentials by considering the disproportionation reaction, which is facilitated by the complexation of Rh_2^{4+} with two supporting electrolyte anions (where $Rh_2 = Rh_2(dimen)_2(dppm)_2$, $Rh_2(dimen)_3(dppm)$, or $Rh_2(dimen)_4$):

$$2Rh_2^{3+} \rightleftharpoons Rh_2^{2+} + Rh_2^{4+} \qquad (1)$$

$$Rh_2^{4+} + 2ClO_4^- \rightleftharpoons Rh_2(ClO_4)_2^{2+} \qquad (2)$$

The expressions (1) and (2) define the following equilibrium constants:

$$K_{disp} = \frac{[Rh_2^{2+}][Rh_2^{4+}]}{[Rh_2^{3+}]^2} \qquad (3)$$

$$K_1K_2 = \frac{[Rh_2(ClO_4)_2^{2+}]}{[Rh_2^{4+}][ClO_4^-]^2} \qquad (4)$$

$$K_{disp}' = K_{disp}K_1K_2[ClO_4^-]^2 = \frac{[Rh_2^{2+}][Rh_2(ClO_4)_2^{2+}]}{[Rh_2^{3+}]^2} \qquad (5)$$

Combining eq 5 with the Nernst equation yields the well-known relationship between the disproportionation constant, K_{disp}', and the two single-electron potentials:[18]

$$\ln K_{disp}' = \frac{nF(E^{\circ\prime}_{3+/2+} - E^{\circ\prime}_{4+/3+})}{RT} \qquad (6)$$

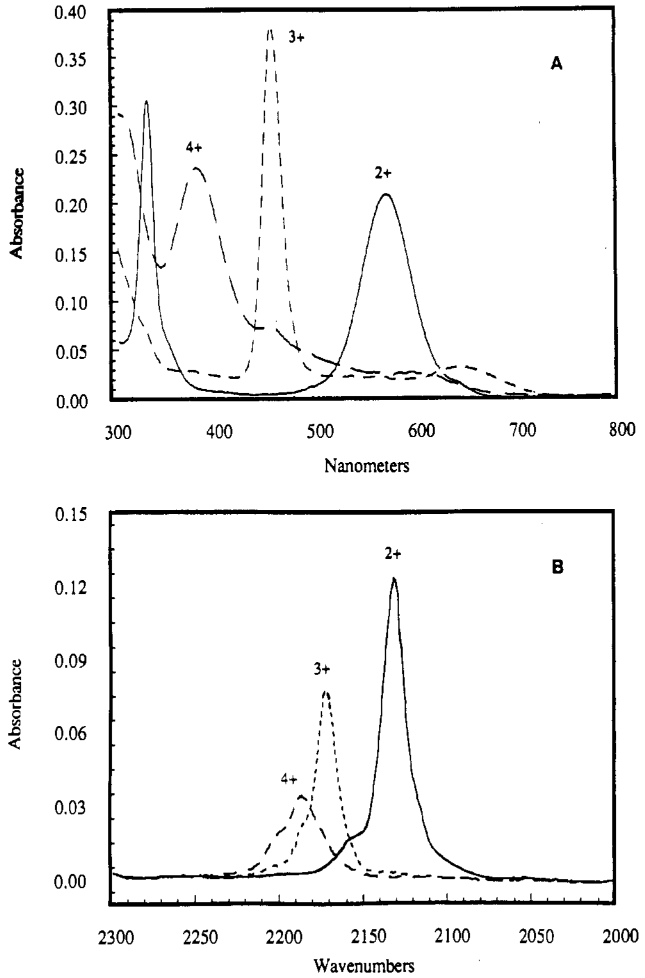

Figure 2. UV–visible (A) and IR (B) spectra of $Rh_2(dimen)_2(dppm)_2^{n+}$ (n = 2–4) recorded before and after sequential bulk electrolyses at +0.9 and +1.5 V.

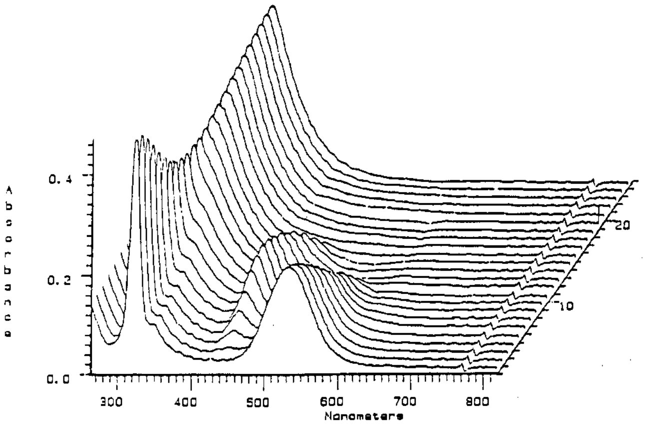

Figure 3. "Waterfall" plot of the UV–visible spectral changes observed during the spectroelectrochemical oxidation of $Rh_2(dimen)_3(dppm)^{2+}$ in 0.1 M $TBA^+ClO_4^-/CH_2Cl_2$.

Measurement of the equilibrium concentrations of the [2+], [3+], and [4+] species generated during a bulk electrolysis allows us to calculate K_{disp}' and, by eq 6, determine the difference between the E° values for the single-electron transfer processes. The potentials of the individual redox couples $E^{\circ\prime}_{3+/2+}$ and $E^{\circ\prime}_{4+/3+}$ can then be determined from the CV data by eq 7.

$$E^{\circ\prime}_{4+/2+} = \frac{E^{\circ\prime}_{3+/2+} + E^{\circ\prime}_{4+/3+}}{2} \qquad (7)$$

Fortunately, the d^8–d^8, d^7–d^8, and d^7–d^7 electronic configurations of binuclear rhodium isocyanide complexes are easily detected by standard spectroscopic methods. Figure 2a,b shows the UV–vis and IR spectra of $Rh_2(dimen)_2(dppm)_2^{n+}$ (where n = 2–4) generated by sequential oxidations at 0.9 and 1.5 V in the spectroelectrochemical cell. Assignments for the d^8–d^8 and d^7–d^8 species have previously been made,[11a] and both the UV–vis and

---

(13) The compound $[Rh_2(dimen)_3(dppm)][PF_6]_2$ is prepared in 80% yield via a modification of the published procedure.[14] Full experimental details will be reported elsewhere.[15]

(14) Mixa, M. M. Ph.D. Thesis, University of Minnesota, 1986.

(15) Hill, M. G.; Mann, K. R. Manuscript in preparation.

(16) Bulk electrolysis of $Rh_2(dimen)_3(dppm)^{2+}$ in 0.1 M $TBA^+ClO_4^-/CH_2Cl_2$ at +1.0 V vs aqueous AgCl/Ag results in the passage of 2.0 (1) electrons.

(17) $E^{\circ\prime}_{3+/2+} = -nF(\Delta G_f(d^7\text{–}d^8) - \Delta G_f(d^8\text{–}d^8))$; $E^{\circ\prime}_{4+/3+} = -nF(\Delta G_f(d^7\text{–}d^7) - \Delta G_f(d^7\text{–}d^8))$. In this treatment, the complexation free energy is included in the $E^{\circ\prime}$ measurements.

(18) Note that, according to eq 6, when the two 1e⁻ potentials are equal ($E^{\circ\prime}_{4+/3+} = E^{\circ\prime}_{3+/2+}$), the disproportionation constant has a value of 1. At 25 °C, for every 59 mV that $E^{\circ\prime}_{4+/3+}$ moves positive of $E^{\circ\prime}_{3+/2+}$, K_{disp}' decreases by a factor of 10; likewise, for every 59 mV that $E^{\circ\prime}_{4+/3+}$ moves negative of $E^{\circ\prime}_{3+/2}$, K_{disp}' increases by a factor of 10. Hence, for a given complex, a large K_{disp}' (>1) indicates that the two 1e⁻ couples are "inverted" ($E^{\circ\prime}_{4+/3+} < E^{\circ\prime}_{3+/2+}$) and a net 2e⁻ oxidation is thermodynamically favored over the corresponding single-electron processes.

Table I. Temperature Dependence of K_{disp}' [a]

$Rh_2(dimen)_2(dppm)_2^{3+}$		$Rh_2(dimen)_3(dppm)^{3+}$		$Rh_2(dimen)_4^{3+}$	
T, °C	$10^{10}K_{disp}'$ [b]	*T*, °C	K_{disp}' [c]	*T*, °C	$10^{-3}K_{disp}'$ [d]
20	8.3 (5)	25	1.04 (18)	25	4.5 (9)
15	5.3 (5)	4	0.94 (40)	10	4.0 (6)
5	2.3 (5)	−10	0.74 (21)	0	3.5 (7)
−1	1.3 (5)	−35	0.71 (22)	−15	2.6 (5)
−3	1.0 (5)	−50	0.53 (33)	−25	2.4 (6)

[a] Standard deviations in the last significant digit are listed in parentheses. [b] K_{disp}' is calculated from the temperature dependence of ($E^{\circ\prime}_{3+/2+} - E^{\circ\prime}_{4+/3+}$) and eq 6. [c] K_{disp}' is determined by UV–vis spectroelectrochemical measurements. [d] K_{disp}' is determined by IR spectroelectrochemical measurements.

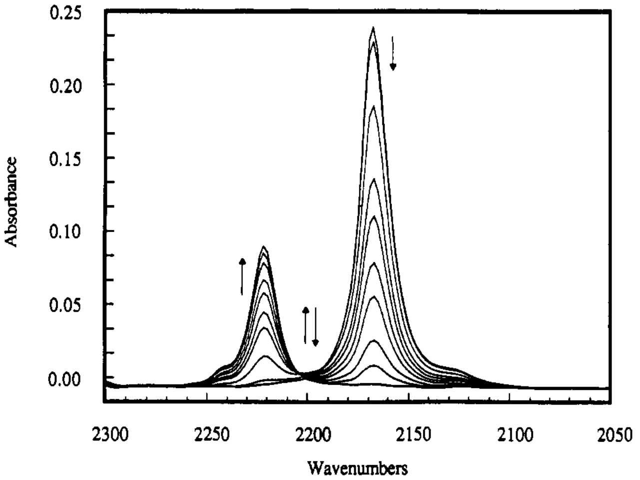

Figure 4. Plot of the IR spectral changes observed during the spectroelectrochemical oxidation of $Rh_2(dimen)_4^{2+}$ in 0.1 M $TBA^+ClO_4^-$/CH_2Cl_2. Note the lack of a distinct isosbestic point at 2200 cm^{-1} where the $Rh_2(dimen)_4^{3+}$ radical absorbs.

IR spectra of the d^7–d^7 species agree well with the spectra of other two-electron oxidized compounds of similar structure.[19]

Figure 3 shows the UV–vis spectroelectrochemical oxidation of $Rh_2(dimen)_3(dppm)^{2+}$; the analogous IR experiment is shown for $Rh_2(dimen)_4^{2+}$ in Figure 4.[20] In each case, the initial spectrum in the series corresponds to the d^8–d^8 starting material, while the final spectrum is attributed to the d^7–d^7 2e$^-$ oxidation product. Note, however, the appearance of transient absorbances (at 430 nm in the UV–vis experiment for $Rh_2(dimen)_3(dppm)^{2+}$ and 2200 cm^{-1} in the IR experiment for $Rh_2(dimen)_4^{2+}$), which increase, reach a maximum value midway through the electrolysis, and eventually disappear. By analogy to the UV–vis and IR spectra of $Rh_2(dimen)_2(dppm)_2^{3+}$ and other d^7–d^8 radicals,[21] these absorbances are assigned to $Rh_2(dimen)_3(dppm)^{3+}$ and $Rh_2(dimen)_4^{3+}$.[22] Plots of the relative concentrations of the d^8–d^8, d^7–d^8, and d^7–d^7 species as a function of the number of electrons removed allow the calculation of radical disproportionation constants at 25 °C of 1.04 (18) for $Rh_2(dimen)_3(dppm)^{3+}$ and 4.5 (9) × 10^3 for $Rh_2(dimen)_4^{3+}$; direct electrochemical data at 20 °C (eq 6) yields a value of 8.3 (5) × 10^{-10} for the disproportionation of $Rh_2(dimen)_2(dppm)_2^{3+}$. Hence, while the second 1e$^-$ oxidation couple ($E^{\circ\prime}_{4+/3+}$) is +0.526 V more positive than the first ($E^{\circ\prime}_{3+/2+}$) for $Rh_2(dimen)_2(dppm)_2^{2+}$, it lies at approximately the same potential as $E^{\circ\prime}_{3+/2+}$ for $Rh_2(dimen)_3(dppm)^{2+}$ and is negative of $E^{\circ\prime}_{3+/2+}$ by more than 0.2 V for $Rh_2(dimen)_4^{2+}$.

Table I summarizes the temperature dependence of K_{disp}', as determined by variable-temperature electrochemical[23] and UV–vis–IR spectroelectrochemical techniques. Van't Hoff plots of these data yield respective values for $\Delta H_{disp}'$ and $\Delta S_{disp}'$ of +14000 cal/mol and +6.6 eu for $Rh_2(dimen)_2(dppm)_2^{3+}$; +1110 cal/mol and +3.8 eu for $Rh_2(dimen)_3(dppm)^{3+}$; and +1930 cal/mol and +23 eu for $Rh_2(dimen)_4^{3+}$. A comparison of the magnitudes of $\Delta H_{disp}'$ and $-T\Delta S_{disp}'$ for each of the three compounds indicates that both enthalpic and entropic factors make significant contributions to the value of K_{disp}'. Moreover, replacing two dimen ligands by two dppm ligands renders the disproportionation reaction enthalpically less favorable by 12 kcal/mol and entropically less favorable by nearly 5 kcal/mol at 25 °C.

Clearly, subtle changes in molecular structure play a key role in directing a given molecule toward multielectron-transfer pathways. At this time, we are investigating the large enthalpy and entropy changes that occur with the sequential replacement of dimen ligands by dppm. These changes must be significant, as K_{disp}' at room temperature encompasses a range of greater than 10^{12}. While in principle these changes can be manifest in any of the d^8–d^8, d^7–d^8, or d^7–d^7 electronic states, our data suggest they result primarily from differences in the thermodynamic stabilities of the various perchlorate bound 2e$^-$ oxidized species. The direction of change in both $\Delta H_{disp}'$ and $\Delta S_{disp}'$ suggests that the pendant phenyl rings of the dppm ligands in the phosphine-substituted complexes interfere with the energetics of the arrangement and subsequent binding of perchlorate ligands to the Rh_2^{4+} cores by partially bloacking the axial sites.

Acknowledgment. We wish to thank Dr. John Bullock for several helpful discussions, Professor J. E. Ellis for the use of his FTIR spectrometer, and Johnson-Matthey, Inc., for a generous loan of rhodium trichloride.

---

[19] (a) Miskowski, V. M.; Smith, T. P.; Loehr, T. M.; Gray, H. B. *J. Am. Chem. Soc.* **1985**, *107*, 7925. (b) Shin, Y.; Miskowski, V. M.; Nocera, D. G. *Inorg. Chem.* **1990**, *29*, 2308.

[20] For experimental details regarding the spectroelectrochemical experiments, see: Bullock, J. P.; Mann, K. R. *Inorg. Chem.* **1989**, *28*, 4006.

[21] Miskowski, V. M.; Mann, K. R.; Gray, H. B.; Milder, S. J.; Hammond, G. S.; Ryason, P. R. *J. Am. Chem. Soc.* **1979**, *101*, 4383.

[22] $Rh_2(dimen)_3(dppm)^{3+}$ exhibits an EPR spectrum very similar to that of $Rh_2(dimen)_2(dppm)_2^{3+}$,[11a] with two signals centered at g = 2.27 and g = 1.99. We have not obtained the EPR spectrum of $Rh_2(dimen)_4^{3+}$.

[23] Values for $E^{\circ\prime}_{3+/2+}$ and $E^{\circ\prime}_{4+/3+}$ were determined for $Rh_2(dimen)_2(dppm)_2^{2+}$ by Osteryoung square-wave voltammetry.

[24] To whom correspondence should be addressed.

Department of Chemistry
University of Minnesota
Minneapolis, Minnesota 55455

Michael G. Hill
Kent R. Mann*[24]

Received October 19, 1990

$[Na_9Fe_{20}Se_{38}]^{9-}$: A High-Nuclearity Bicyclic Cluster Constructed by the Fusion of Fe_2Se_2 Rhombs

The syntheses of high-nuclearity metal–oxide, –chalcogenide, and –pnictide clusters in soluble molecular forms[1-6] and within

---

[1] Schmid, G. *Struct. Bonding (Berlin)* **1985**, *62*, 51.

[2] Kharas, K. C. C.; Dahl, L. F. *Adv. Chem. Phys.* **1988**, *70* (2), 1.

[3] (a) Fenske, D.; Ohmer, J.; Hachgenei, J.; Merzweiler, K. *Angew. Chem., Int. Ed. Engl.* **1988**, *27*, 1277. (b) Fenske, D.; Hollnagel, A. *Angew. Chem., Int. Ed. Engl.* **1989**, *28*, 1390.

[4] (a) Lippard, S. J. *Angew. Chem., Int. Ed. Engl.* **1988**, *27*, 344. (b) Micklitz, W.; Lippard, S. J. *J. Am. Chem. Soc.* **1989**, *111*, 6856.

0020-1669/91/1330-1431$02.50/0 © 1991 American Chemical Society